LA-8298-PR

Progress Report

C.3

Applied Nuclear Data Research and Development

October 1—December 31, 1979

LOS ALAMOS SCIENTIFIC LABORATORY
Post Office Box 1663 Los Alamos, New Mexico 87545

The four most recent reports in this series, unclassified, are LA-7722-PR, LA-7843-PR, LA-8036-PR, and LA-8157-PR.

The report was not edited by the Technical Information staff.

This work was performed under the auspices of the US Department of Energy's Office of Military Application, Division of Reactor Research and Technology, Office of Basic Energy Sciences, and Office of Fusion Energy; and the Electrical Power Research Institute.

UNITED STATES
DEPARTMENT OF ENERGY
CONTRACT W-7405-ENG. 36

LA-8298-PR
Progress Report
UC-34c
Issued: March 1980

Applied Nuclear Data Research and Development

October 1—December 31, 1979

Compiled by
C. I. Baxman and P. G. Young

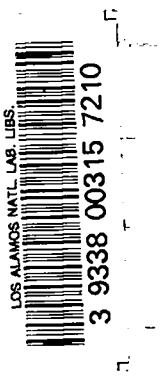

CONTENTS

APPLIED NUCLEAR DATA RESEARCH AND DEVELOPMENT
QUARTERLY PROGRESS REPORT
October 1 - December 31, 1979

Compiled by

C. I. Baxman and P. G. Young

ABSTRACT

This progress report describes the activities of the Los Alamos Nuclear Data Group for the period October 1 through December 31, 1979. The topical content is summarized in the contents.

I. THEORY AND EVALUATION OF NUCLEAR CROSS SECTIONS

A. Low-Energy Behavior of Fusion Cross Sections (G. M. Hale and D. C. Dodder)

The low-energy behavior of fusion cross sections is very important for determining the reaction rates for light ions confined at low temperatures. Measurements of these cross sections in the few-keV to tens-of-keV range are quite difficult, mainly because the yields are so low and vary so rapidly with energy that precise determinations of the relative beam-target energies are required. Therefore, simple expressions based on Coulomb barrier penetration have been used in previous studies to extrapolate the cross sections from the region where they can be measured reliably to low energies.

These extrapolations generally have the form

$$\sigma_{c'c}(E) = S_{c'c}(E)\,\tilde{P}_c(E) \quad , \tag{1}$$

where $\tilde{P}_c(E)$ is an approximation to the Coulomb penetrability factor (the most familiar being the Gamow factor $e^{-b/\sqrt{E}}$) in the entrance channel c, and $S_{c'c}(E)$

(sometimes called the "astrophysical S-function") is presumed to account for nuclear effects in the cross sections. In practice, the S-function is often taken to be constant at low energies.

R-matrix theory gives the rigorous result for low-energy cross sections

$$\sigma_{c'c}(E) = \frac{1}{E} S_{c'c}(E)\, P_c(E) \quad , \tag{2}$$

where $P_c(E)$ is the entrance-channel Coulomb penetrability factor defined in terms of the outgoing Coulomb spherical wave, $O_c(ka)$, as $P_c = \frac{ka}{|O_c(ka)|^2}$, and the S-function is given by

$$S_{c'c}(E) \sim P_{c'}(E) \quad |R^L_{c'c}(E)|^2 \quad . \tag{3}$$

Here $P_{c'}(E)$ is the exit-channel Coulomb penetrability and $R^L_{c',c}$ is the s-wave R-matrix element defined for the (complex, energy-dependent) boundary conditions

$$B_c = L_c \equiv a_c \frac{\partial O_c}{\partial r_c} \; / \; O_c \; | \; r_c = a_c \quad , \tag{4}$$

at the channel radii a_c. Note that the R-matrix expression (3) for the S-function contains Coulomb effects explicitly in addition to nuclear effects.

We have calculated the S-functions at low energies resulting from our R-matrix analyses of the 4- and 5-nucleon systems for two of the important fusion reactions, $T(d,n)^4He$ and $D(d,n)^3He$. These calculations, shown in Figs. 1 and 2, use the approximate Gamow penetration factor in order to compare with what is more commonly done. It is clearly evident that the S-functions for these reactions do not behave as constants at low energies. However, Arnold et al.[1] reported values of the T(d,n) cross section obtained with the assumption of constant S in place of their own measurements at energies below 20 keV. This is the horizontal dashed line labeled "Gamow extrapolation" in Fig. 1. The R-matrix extrapolation (solid curve) is more consistent with their original measurements.

The 40% change in the S-function for the T(d,n) reaction in the 0-30 keV range is not surprising in view of the large S-wave resonance situated at approximately 100 keV. However, the 14% change in the D(d,n) S-function for energies up to 50 keV is somewhat unexpected and appears to come mainly from the 0^+ level located at a few MeV below the d + d threshold.

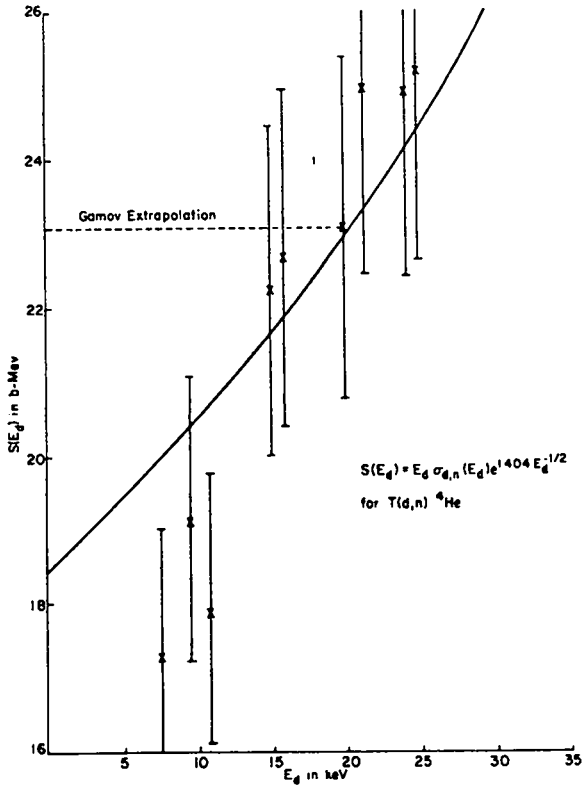

Fig. 1.
Calculated S-function for the $T(d,n)^4He$ reaction compared to the measurements and Gamow extrapolation of Arnold et al.[1] at energies below 30 keV.

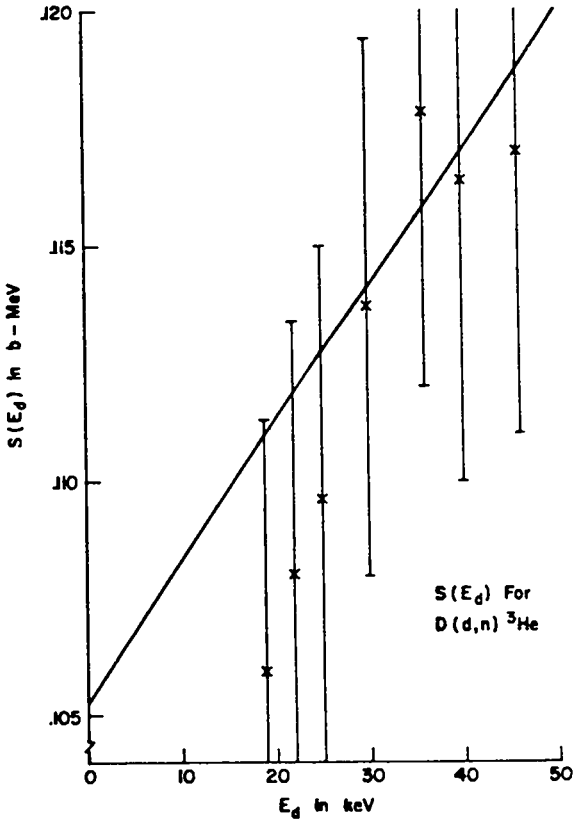

Fig. 2.
Calculated S-function for the $D(d,n)^3He$ reaction at energies below 50 keV compared to measurements from Ref. 1 that have been corrected for changes in the assumed D(d,n) angular distributions.

B. Calculations of Neutron Cross Sections for ^{59}Co up to 40 MeV [W. K. Matthes (EURATOM, Ispra) and E. D. Arthur]

The $^{59}Co(n,p)$, (n,2n), (n,3n), and (n,4n) reactions have been proposed as suitable candidates to satisfy dosimetry needs for materials irradiation in the high-energy neutron flux of the Fusion Materials Irradiation Test Facility (FMIT). Since no experimental data for these reactions exist above 24 MeV, we have begun nuclear-model calculations of needed cross-section data up to 50 MeV. Our approach is similar to one followed in our recent calculations of high-energy neutron reactions on iron.[2]

Initially we have begun a search to find input parameters suitable for use over the entire energy range of the calculation. Our main effort to date has been the determination of spherical neutron optical parameters through fits to resonance information, total and reaction cross sections, and elastic angular distributions, the results of which are presented in Table I. These parameters can be used up to energies of 50 MeV while displaying reasonable low-energy behavior so that (n,xn) reactions can be accurately calculated. For the present, proton and alpha-particle transmission coefficients have been calculated using modified versions of parameter sets[3,4] used for our n + Fe calculations. In addition, gamma-ray strength functions for cobalt compound nuclei have been determined from fits to neutron capture data. We have also updated our discrete level files using recent level information[5] along with adjustment of level-density parameters to better reproduce s-wave resonance spacing data. Preliminary calculations of direct effects in inelastic scattering from the first few levels in ^{59}Co have been made assuming the applicability of the weak coupling model[6] to this odd-A nucleus. Under this model, the presumption is made that the presence of a spin 7/2 hole (in this case) outside a spherical core (^{60}Ni) does not affect the collective vibration of the core. We made DWBA calculations of inelastic scattering from the 2^+ state (1.33 MeV) in ^{60}Ni using the optical parameters of Table I and $\beta_2 = 0.2$ and then apportioned the calculated direct cross section between low-lying states in ^{59}Co having spins from 3/2 to 11/2. Efforts are now underway to make preliminary comparisons to measured results for inelastic scattering below 4 MeV and to other data for (n,p), (n,2n), and (n,3n) reactions. Once satisfactory results are obtained, we will extend the calculation to 50 MeV.

C. Calculation of Prompt Fission Neutron Spectra [D. G. Madland and J. R. Nix (T-9)]

The status of the prompt fission neutron spectrum calculations has been summarized at the recent International Conference on Nuclear Cross Sections for Technology.[7]

Work has continued on calculations using energy-dependent compound-nucleus formation cross sections generated from various neutron-nucleus optical potentials. Comparisons are being made to experimental prompt neutron spectrum data from several differing fissioning systems. Possible modifications of the

TABLE I

NEUTRON OPTICAL PARAMETERS FOR ^{59}Co

	r(fm)	a(fm)
$V(MeV) = 47.604 - 0.364E - 0.0003E^2$	1.2865	0.561
$W_{vol}(MeV) = -0.072 + 0.148E$	1.3448	0.473
$V_{SO}(MeV) = 6.2$	1.12	0.47
$W_{SD}(MeV) = 8.047 + 0.08E$	1.3348	0.473
Above 6 MeV		
$W_{SD}(MeV) = 8.53 - 0.251\ (E-6)$	1.3348	0.473

present calculations due to multiple-chance fission effects at high-incident neutron energy are under study.

Calculations of the average number of prompt neutrons per fission ν_p, using the formalism developed for the fission spectrum calculations, have been performed for ^{252}Cf (sf) and for the $^{233,235,238}U$ (n,f) and $^{239,240}Pu$ (n,f) reactions at various incident neutron energies. The results compare well with experimental measurements. Additional calculations and comparisons are continuing.

D. Medium Energy Library (D. G. Foster and D. M. McClellan)

The Los Alamos Scientific Laboratory (LASL) Medium-Energy Library (MEL) of Monte-Carlo histories[8] has been transferred from photostore to the Common File System (CFS), except for 11 data sets that were found to be missing. CROS checksums were verified after converting to LTSS monitor mode if there were checksums on the photostore copies. We have also taken advantage of the move to correct some systematic errors in the data or file structure and have appended CROS-like checksums to all of the CFS data sets.

All MEL data sets are in the Green partition with universal read access. A given set is described by its target nuclide, incident particle, and incident energy, attached in that order to a root directory /MEDENL. Thus, for example, the data for 100-MeV protons incident on Fe can be retrieved via the path /MEDENL/FE/PRO/100. The entire library comprises 19 particle-target

combinations for 11 elements spanning the range from carbon to ^{238}U ("U238"). It contains 239 data sets altogether, representing roughly 60 hours of CDC 7600 time.

The surviving contents of the library are summarized in Table II. The numbers in the body of the table are version designations for the intranuclear-cascade + evaporation code CROIX[8-10] that were used to generate the Monte-Carlo histories stored in the MEL. These versions are also recorded in an INFO entry accompanying each set. An additional CFS node /MEDENL/SUMMARY contains a chart of the complete tree. It lists the version and the numbers of interactions and transparancies (where these were available) in the corresponding data set. The legend accompanying the table summarizes the principal characteristics of the successive versions but does not mention that a major revision of the EVAP section of CROIX occurred[10] between versions 3 and 4. The sets MO/PRO/100 and U238/NEU/800 are hybrids formed by combining old tapes; they are upward compatible in the sense that the entire file can be read using the older of the two formats. Since the physics incorporated into CROIX changed between versions 3 and 4, FE/NEU contains sets 60 and 60A, respectively, in order to permit comparison of the effects of the changes.

II. NUCLEAR CROSS SECTION PROCESSING

A. Cross Sections for Neutron Transport (R. E. MacFarlane and R. M. Boicourt)

The MATXS/TRANSX system is a convenient and flexible tool for storing and retrieving multigroup cross sections for neutron transport codes. The MATXS file is capable of storing neutron cross section, photon production data, and photon interaction cross sections. It can include self-shielded cross sections, fission matricies, heat production (KERMA) factors, material damage production cross sections, and thermal scattering data.

MATXS files are converted into forms acceptable to many neutron transport codes using the TRANSX code. A new version of this code is now available that has the following capabilities: it will produce neutron tables, photon tables, or coupled sets in direct or adjoint form and in materialwise or groupwise ordering; tables can be written in card format, FIDO format, ISOTXS format, or a new group-ordered binary format; transport corrections can be applied, prompt or steady-state fission $\bar{\nu}$ and spectra can be retrieved; tables may be collapsed to a subset group structure; thermal upscatter may be included for low energy

TABLE II

MONTE-CARLO HISTORIES IN THE MEDIUM-ENERGY LIBRARY
(Particle Energy, MeV)

Target	Particle	15	20	25	33	42	50	60	100	125	200	300	400	500	600	700	800	1000	1500	2500	3500
C-12	n	1	1	1	4	4	1	4	1	4	1	1		1	1	1	1				
	p	1	4	4			4		4		4	4	4	4	4	4	4	4	4	4	4
N-14	n		4	4	4	4	4	4	4	4											
O-16	n	1	1	1	4	4	4+	4	1	4	1	4+	1	4+	1	1	4				
	p	1	4	4			4		4		4	4	4	4	4	4	4		4	4	4
AL-27	n	1	1	1					1		1	1	1	1		1	1				
	p		4	4+			1		1		1	1	4+	1	4+	1	1	4	4+	4	4
Si-28	n		1	1	4	4	1	4+	1		1	1	1	1	1	1	1				
Fe	n	1	1	1	3	3	1	3,4	1		1	1	1	1	1	3	1				
	p	1	4+	4+			4+		4+		2	2	2	2	2	2	2	4	4	4	4
Cu	n	1	1	1			1		1			1			1	1	1				
	p	1		1			1		1		1	1	1	1	1		1				
Mo	n		1	3			3		1		3	3	3	1	3	3	1				
	p			3			3		2		2,1	2	2	2	2	3	3				
W	n		1	3	4	3	3		1		3	3	1	1	3	3	3				
	p			3			3		3		3	3	3	3	3	3	3				
Pb	n	1	1	1			1		1		1	1	1	1	1	1	1				
U-238	n	1	1	1			1		1		1	1	1	1	1	1	3,1				
	p	1	1	1			1		1		1	1	1	1	1	1	1				

Legend:
1. No additional data
2. Add data on final residual nucleus
3. Add data on intermediate and final residual nuclei
4. Add data on intermediate and final residual nuclei plus heavy particles
4+. Same as 4 but using EVAP-4 instead of EVAP-3

groups; isotopes can be mixed to form microscopic or macroscopic cross sections including self-shielding for homogeneous systems (infinite or buckled), simple spherical or cylindrical systems, or multiple slab periodic cells; and very general response functions can be constructed that are any linear combination of cross sections from the library.

This code and several cross-section libraries are available on the LASL-7600's and also at the National Magnetic Fusion Energy Computer Center (MFECC) at Lawrence Livermore Laboratory (LLL). The file names and descriptions follow.

LASL	MFECC
/TRANSX/S2	(5005) TRANSX

Source code for TRANSX including input instructions.

/TRANSX/X2	(5005) TRANSXX

Executable binary version of TRANSX

/TRANSX/MATXS1	(5005) MATXS1

A 30 neutron group by 12 photon group library from ENDF/B-IV at 300K and infinite dilution.

/TRANSX/MATXS5	(5005) MATXS5

A similar library from ENDF/B-V.

/TRANSX/MATXS6	(5005) MATXS6

A 70 by 12 library from ENDF/B-V designed for fast reactor problems and including self-shielding for many temperatures and background cross sections.

/TRANSX/MATXS7	(5005) MATXS7

A 69 neutron group ENDF/B-V library for thermal reactor analysis including thermal data for several moderators and self-shielded data for the actinides.

(Not Available)	(5005) TRANSIN

Sample problem input decks for TRANSX.

/MATX/BBC/0	(5005) BBC

Source code for BBC that can convert MATXS files between BCD and binary modes, list the cross sections, or index the file by material and reaction type.

/MATX/BBC/OX (5005) BBCX

Executable binary code for BBC.

This system of codes and libraries is capable of giving accurate results for a wide variety of thermal-reactor, fast-reactor, shielding, and fusion-reactor problems.

B. LIB70 (R. B. Kidman)

A 43-isotope, 70-group library was generated and distributed to several laboratories last quarter. Since then, R. E. MacFarlane has discovered and fixed an error that affects the transport f-factor. In order to test the effects of the fix, multigroup constants for the following isoptopes were regenerated: C, ^{16}O, ^{23}Na, ^{27}Al, Cr, ^{55}Mn, Fe, Ni, ^{232}Th, ^{235}U, ^{238}U, ^{239}Pu, ^{240}Pu, and ^{242}Pu. The new library lowers the ZPR-6-7 and ZPR-6-6A eigenvalues by 0.27%.

This change is not large nor does it seem entirely negligible. Therefore, it is not obvious if we should regenerate the rest of the isotopes and send out a new library. The most prudent route may be to wait and see if more errors are discovered before we take the time and expense to regenerate the library.

Some of the salient parameters from our assigned Phase II calculations (using the new library) are presented in Table III.

TABLE III

	Uncorrected Eigenvalues	Central Reaction Rate Ratios		
		F^{28}/F^{25}	F^{49}/F^{25}	C^{28}/F^{25}
JEZEBEL	1.0055	0.1996	1.4087	0.0663
GODIVA	1.0013	0.1705	1.3925	0.0713
ZPR-6-7	0.9820	0.0228	0.9456	0.1463
ZPR-6-6A	0.9800	0.0241	0.9786	0.1455

C. Thermal Power Reactor Isotopics (R. E. MacFarlane)

The Electric Power Research Institute (EPRI) reactor fuel cycle code EPRI-CELL is now used widely by the electric utilities and the national laboratories. As part of a program to adapt EPRI-CELL to use the latest evaluated nuclear data set ENDF/B-V, a new isotopics module has been written and two new burn libraries have been prepared.

The original burn calculation in CELL was based on the CINDER code and vintage 1965 libraries.[11] Since this time, extensive work has been performed to improve and extend libraries of actinide and fission-product decay data, cross sections, and yields culminating in the ENDF/B-V set soon to be released. Cross sections from ENDF/B-V are now available for use in the GAM/THERMOS flux calculation of CELL; it is therefore important to update the burn library to correspond.

The existing burn module coding in CELL is library dependent and makes inefficient use of storage. Since it is very desirable to be able to change burn libraries for different purposes without having to make code changes, it was decided to extensively recode the isotopics module. In the process, a new library format was defined, variable-dimensioned storage was improved, a new method was adopted to solve the chain equations, a decay-heat calculation was implemented, and the coding was divided into more subroutines for improved readability.

The new library format stores cross sections, yields, decay constants, and decay-heat values by real isotope rather than linear isotope. This prevents the repetition of data found in earlier EPRI-CELL-CINDER libraries. To give equivalent flexibility, explicit branching factors are used, and the format allows for any number of reaction types as long as they add up to the total absorption cross section. This scheme allows for any type of chain continuation to be indicated explicitly (i.e., decay, nγ, n,2n, etc.). The new format allows for any number of groups; zero cross sections below thresholds are suppressed. Finally, any number of fission precursors are allowed for the yield tables. The new library format is generated from a free-form card input that makes heavy use of alphanumeric phrases such as "TH232" or "N2N", which are easy for the user--they are converted into numbers and pointers that are easy for the computer to read by a library utility code BLIB.

The nuclide densities in the reactor fuel are represented by the linearized chains described by the coupled differential equations[12]

$$\frac{dNi}{dt} = Y_i + G_{i-1}N_{i-1} - B_iN_i \quad , \tag{5}$$

where the N_i are number densities, Y_i are fission-product yield rates, G_{i-1} are production rates from the previous nuclide in a chain ($G_0=0$), and B_i are isotope destruction rates. The general solution to these equations is

$$N_i(t) = \alpha_i + \sum_{j=1}^{i} \beta_{ij}\, e^{-B_j(t-t_0)} \quad . \tag{6}$$

It is convenient to write this in the form

$$N_i(t) = N_i(t_0)\, e^{-B_i(t,t_0)} + Y_i \left[\frac{1-e^{-B_i(t-t_0)}}{B_i}\right]$$

$$+ G_{i-1} \left\{\alpha_{i-1} \left[\frac{1-e^{-B_i(t-t_0)}}{B_i}\right]\right.$$

$$\left. + \sum_{j=1}^{i-1} \beta_{i-1,j} \left[\frac{e^{-B_j(t-t_0)} - e^{-B_i(t-t_0)}}{B_i - B_j}\right]\right\} \quad , \tag{7}$$

where the coefficients are defined recursively

$$\alpha_1 = Y_1/B_1 \quad ,$$

$$\alpha_i = (Y_i+G_{i-1}\alpha_{i-1})/B_i \quad , \quad i > 1 \quad ,$$

$$\beta_{11} = N_1(t_0) - Y_i/B_1 \quad ,$$

$$\beta_{ij} = G_{i-1}\beta_{i-1\ j}/(B_i-B_j) \quad , \quad i > 1,\ j < i \quad ,$$

$$\beta_{ii} = N_i(t_0) - \alpha_i - \sum_{j=1}^{i-1} \beta_{ij} \quad , \ i > 1 \quad . \tag{8}$$

This form is very economical of storage. The factor in curly brackets can lose significance, so it is set to zero if its magnitude is much smaller than the magnitude of its largest term. As in the original coding, production and destruction rates are computed using CELL fluxes with self-shielded and flux-dependent cell cross sections for isotopes named in the flux calculation and coarse-group cross sections from the burn library for any other isotopes.

The original EPRI-CELL contains inactive coding for calculating decay heat by explicitly summing the decays from each isotope. This type of calculation is not useful at power or close to shutdown because the libraries used do not include the many short-lived nuclides that dominate the equilibrium decay heating by fission products (the explicit calculation can be made accurate for the actinides at short times by including only a few short-lived isotopes[13]). As an example, the 84-chain EPRI-CINDER library[12] gives accurate decay-heat predictions for cooling times greater than approximately 20 hours. This problem can now be solved by using the new standard for decay heat[14] that represents the decay heat as a function of cooling time after a fission burst in the form

$$f(t) = \sum_{i=1}^{23} \alpha_i e^{-\lambda_i t} \quad , \tag{9}$$

in units of MeV/sec/fission. If absorption effects are neglected, the burst function can be folded into a power history represented as F(t) in fissions/sec/atom to give the decay heat in MeV/sec/atom

$$H(t) = \sum_i h_i e^{-\lambda_i (t-T)} \quad , \tag{10}$$

where T is the shutdown time, t is greater than T, and the power-history dependent coefficients are given by

$$h_i = \alpha_i \int_0^T F(t')f(t-t')dt' \quad . \tag{11}$$

Assuming that F is constant for each time step $t_j \leq t \leq t_{j+1}$,

$$h_i = \alpha_i \sum_j F_j \frac{e^{-\lambda_i (T-t_{j+1})} - e^{-\lambda_i (T-t_j)}}{\lambda_i} \quad . \tag{12}$$

For use in EPRI-CELL, it is convenient to represent this by a recursion relation using $\Delta t_j = t_{j+1} - t_j$. Starting with $T = 0$ and $h_0 = 0$,

$$T \leftarrow T + \Delta t_j \quad ,$$

$$h_i \leftarrow e^{-\lambda_i \Delta t_j} h_i + \alpha_i F_j \left[\frac{1-e^{-\lambda_i \Delta t_j}}{\lambda_i} \right] \quad . \tag{13}$$

Thus, $\sum_i h_i$ is the fission product decay heating rate that would be observed if the reactor were shut down at the end of the time step. The subsequent cooling curve can then be computed using Eq. (10).

For initial testing of the new EPRI-CELL burn module, the burn libraries have been constructed based on the ENDF/B-IV libraries of EPRI-CINDER. The bigger library contains 84 fission-product chains (188 different isotopes, 487 linear nuclides) and 9 actinide chains (27 isotopes, 68 linear nuclides). It is fairly accurate for fission-product densities and heating from about 20 hours to 3000 years and actinide densities and heating for uranium and thorium cycles at times up to 3000 years. The smaller library is based on the 12-chain reduced set with two chains added to allow "normal samarium" (i.e., the part of the ^{149}Sm density arising directly from ^{149}Pm yields) to be separated out for consistency with subsequent codes. The final library contains 14 fission-product chains (32 real, 48 linear) and 8 actinide chains (20 real, 52 linear). This compact library is designed to represent the fission product and actinide absorption as a function of time. Explicit densities should not be used, and the decay heat has been set to zero to remove temptation. Note that burst functions for ^{232}Th and ^{233}U are not yet available.

The two new libraries have been compared to the standard library for a typical pressurized water reactor (PWR) fuel rod. All three runs used ENDF/B-V cross sections for the flux calculation part of the EPRI-CELL runs. Table IV compares run time and storage requirements. Figure 3 compares total fission product absorption (i.e., normal ^{135}Xe + normal ^{149}Sm + epithermal lump + thermal lump), and Figs. 4 and 5 compare the separate thermal and epithermal lumped absorbers. The decay-heat calculation has been tested by shuting the reactor down at 2000 hours (see Table V). Note that the "standard" and "explicit" fission product decay-heat calculations converge after 20 hours of cooling. Also note the important contribution of the actinides. These results are consistent with EPRI-CINDER and CINDER-10 analyses of the TMI-2 accident.[13]

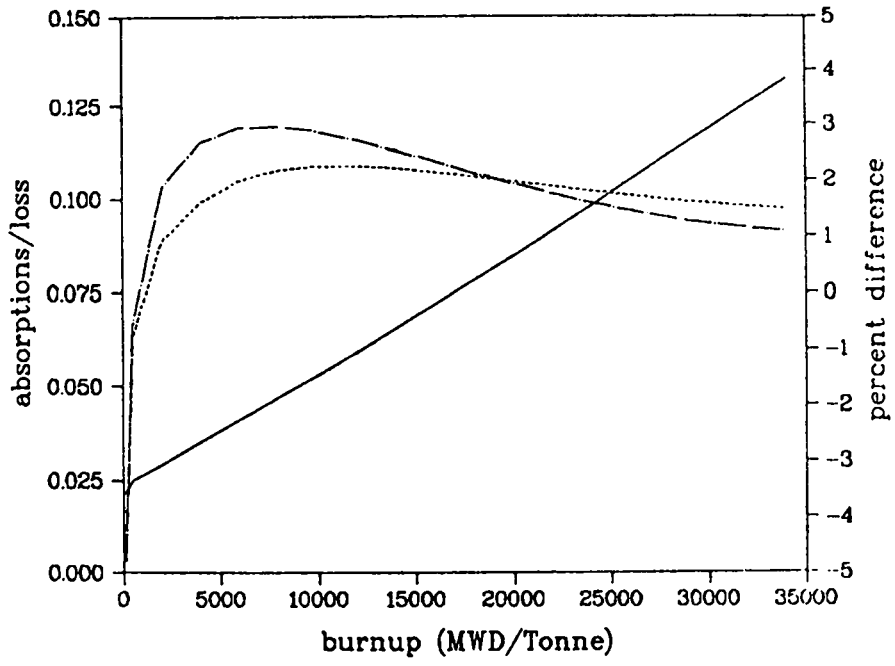

Fig. 3.
Total fission product absorption for a PWR fuel pin by three different methods: (solid line) standard EPRI-CELL code absorption per neutron loss (left scale); (dashed line) per-cent difference between new 84-chain result and standard result (right scale); (dot-dash line) per-cent difference between new 14-chain result and standard result (right scale).

TABLE IV

COMPARISON OF RUN TIME AND STORAGE REQUIREMENTS
FOR THE NEW EPRI-CELL BURN MODULE WITH THE STANDARD CODE

Code Version	Storage Used	Time per Cycle (s)
Standard EPRI-CELL	17040	2.5
New code big library	7670	1.3
New code small library	1530	0.47

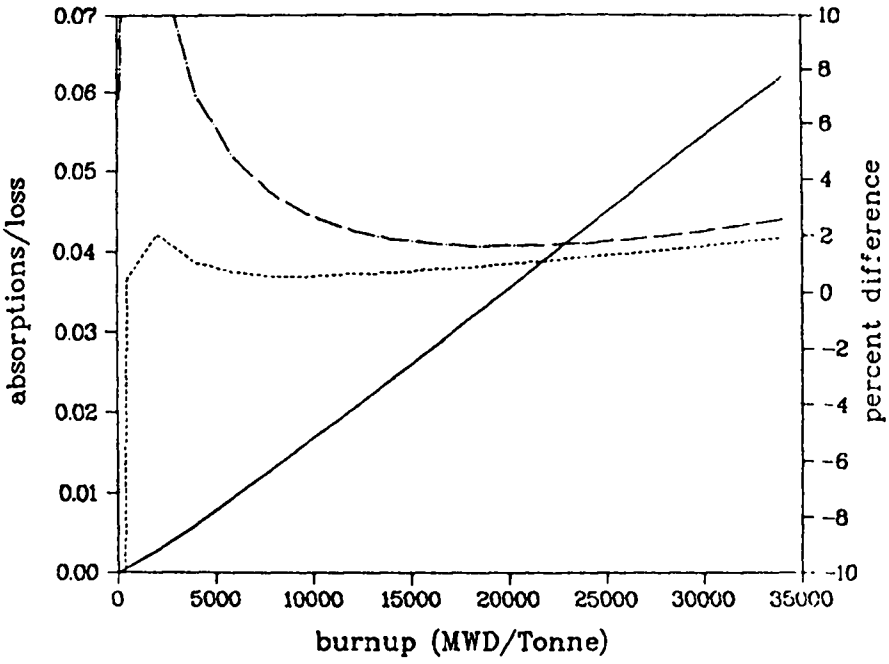

Fig. 4.
Comparison of epithermal lump absorption by three methods: (solid line) standard EPRI-CELL code absorption per neutron loss (left scale); (dashed line) per-cent difference between new 84-chain result and standard result (right scale); (dot-dash line) per-cent difference between new 14-chain result and standard result (right scale).

TABLE V

DECAY HEAT CALCULATIONS USING NEW EPRI-CELL BURN MODULE FOR A PWR FUEL PIN AFTER 2000 h AT 187 W/cm

Cooling Time (h)	Standard Fiss.Prod. (W/cm)	Explicit Fiss.Prod. (W/cm)	Explicit Actinides (W/cm)
0.0	46.12	----	1.872
0.1	15.90	4.329	1.713
1.0	8.251	4.100	1.052
5.0	4.650	3.719	0.843
20.0	2.785	2.699	0.702
100	1.566	1.560	0.265
1000	0.4266	0.4278	0.00018
5000	0.0840	0.0838	0.00008
12000	0.0282	0.0281	0.00008

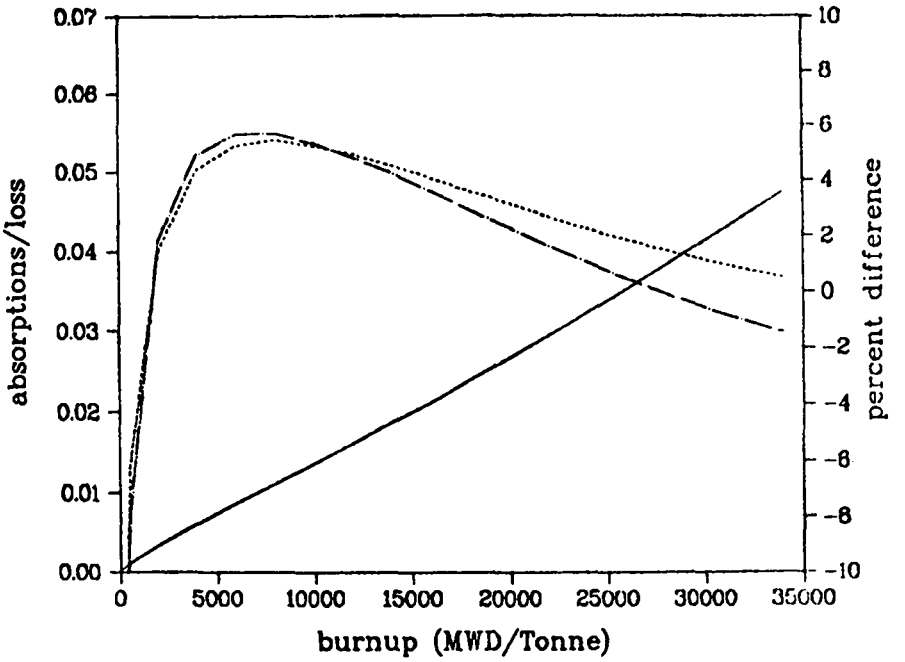

Fig. 5.
Comparison of thermal lump absorption by three methods: (solid line) standard EPRI-CELL code absorption per neutron loss (left scale); (dashed line) per-cent difference between new 84-chain result and standard result (right scale); (dot-dash line) per-cent difference between new 14-chain result and standard result (right scale).

These additions and refinements coupled with new ENDF/B-V libraries to be produced soon make EPRI-CELL useful for either (1) fast and economical flux history calculations using few-chain burn libraries, or (2) detailed heating and isotopics calculations useful for loss-of-coolant accidents, interim storage, reprocessing, and ultimate geological disposal.

III. FISSION PRODUCT AND ACTINIDES: YIELDS, DECAY DATA, DEPLETION, AND BUILDUP

A. Delayed Neutron Data and Calculations (T. R. England, W. B. Wilson, and N. L. Whittemore)

Delayed neutrons per fission and spectra have been calculated using ENDF/B-V fission yields and emission probabilities (Pn), revised from the measured values in Ref. 15, and spectra from individual precursors. The spectral calculations are still in progress, but the preliminary equilibrium ^{235}U spectra are compared with the ENDF/B-V evaluation in this section.

There are approximately 105 precursors based on energetics. Of these, 67 have measured Pn values. These 67 account for approximately 93% of the total delayed neutrons emitted in ^{235}U fission. The calculations use the 67 measured Pn's and simple model estimates for the 38 unmeasured precursor values. The measured values are those evaluated during the IAEA Specialists' Meeting in March 1979.[16]

Table VI lists the 105 precursors and Pn values, including the model estimates; the estimated values are those having no tabulated uncertainty. Also listed in Table VI are the calculated fractional contributions to the total $\bar{\nu}_d$ for ^{235}U thermal fission.

Table VII shows a comparison of $\bar{\nu}_d$ calculated for 20 yield sets in ENDF/B-V with evaluated ENDF/B-V values, a recent evaluation by Tuttle,[16] and selected experimental data. The calculations are in reasonable agreement with evaluations for approximately 15 of the 20 comparisons. Uranium-238 fast fission is <u>not</u> in agreement; the reason appears more likely due to errors in fission yields than to errors in Pn values. Additionally, errors in the yield distribution parameters (pairing effects, most probable charge, etc.) are more likely than errors in the mass chain yields. This work is continuing as one aspect in the process of fission-yield evaluation. However, it now appears that some relatively small improvements in fission yields and Pn values will permit accurate $\bar{\nu}_d$ calculations for all yield sets. The improved data could result from data adjustment methods as noted in Ref. 17; this reference describes the information in Tables VI and VII in more detail.

The spectra for 24 individual precursors were recently supplied by Gösta Rudstam[18] from Studsvik. These are in 10-keV bins and extend from 0 to approximately 3 MeV, depending on the precursor. Below approximately 30 keV, spectra have been estimated by Rudstam, as were some high-energy values. The measured spectra exceed 90% of the total spectra in most cases and average to greater than 90% over all 24 nuclides.

The spectra have been combined using a weighting by the ENDF/B-V yields and the Pn values of Table VI to produce an equilibrium spectrum. The ^{235}U result, compared with the ENDF/B-V evaluation, is shown in Fig. 6. The large calculated peak at approximately 15 keV has been experimentally verified.

The calculated spectra for ^{235}U show peaks at the following energies (up to 1 MeV): 15, 95, 135, 185, 225, 255, 315, 375, 425, 475, 505, 575, 645, 685,

TABLE VI

DELAYED NEUTRON PRECURSORS

	PRECURSOR CS ZZAAAS	HALF-LIFE (s)	Pn (%)	NO. OF SPEC MEAS	% of $\bar{\nu}_d$ U235(T)
	Zn 300790	2.74	1.1	0	< 0.01
	Ga 310790	3.00	0.102±0.015[a]	1	< 0.01
C	Ga 310800	1.66	0.87 ±0.05[a]	1	< 0.01
C	Ga 310810	1.23	12.2 ±0.9[a]	1	0.05
C	Ga 310820	0.60	21.0 ±1.4[a]	0	0.08
	Ga 310830	0.31	56.0	0	0.01
	Ge 320830	1.9	0.17	0	< 0.01
	Ge 320840	1.2	10.0	0	0.18
	Ge 320850	0.234	20.0	0	0.05
	Ge 320860	0.259	22.0	0	0.01
	As 330840	5.6	0.13 ±0.06	0	0.02
	As 330850	2.03	22.0 ±8.0[b]	4	1.94
	As 330860	0.9	10.5 ±2.2	0	0.53
	As 330870	0.73	44.0 ±14.0	0	1.72
	Se 340870	5.60	0.19 ±0.03[b]	0	0.08
	Se 340880	1.52	0.5 ±0.3[b]	0	0.10
	Se 340890	0.41	5.0 ±1.5	0	0.34
	Se 340900	0.555	11.0	0	0.15
	Se 340910	0.27	21.0 ±8.0	0	0.02
C	Br 350870	55.7	2.54 ±0.10[b]	6	2.88
C	Br 350880	16.0	6.9 ±0.3[b]	1	7.96
C	Br 350890	4.38	13.9 ±1.0[b]	2	10.38
C	Br 350900	1.92	21.2 ±2.4[b]	2	8.18
C	Br 350910	0.542	10.9 ±1.8[b]	1	1.51
	Br 350920	0.362	22.0 ±6.0	0	0.45
	Br 350930	0.201	41.0	0	0.07
	Kr 360920	1.85	0.033±0.003	0	0.03
	Kr 360930	1.29	1.95 ±0.11[b]	0	0.58
	Kr 360940	0.208	5.7 ±2.2[b]	0	0.71
	Kr 360950	0.50	9.5	0	0.04
	Rb 370920	4.53	0.0119±0.0006[b]	1	0.03
C	Rb 370930	5.86	1.37 ±0.08[b]	3	2.79
C	Rb 370940	2.76	10.3 ±0.5[b]	4	10.41
C	Rb 370950	0.384	8.8 ±0.4[b]	3	4.07
	Rb 370960	0.201	13.9 ±0.7[b]	1	1.62
	Rb 370970	0.170	27.8 ±2.5[b]	2	1.23
	Rb 370980	0.119	16.0 ±1.0[b]	1	0.02
	Rb 370990	0.076	15.0 ±3.0[a]	0	< 0.01
	Sr 380970	0.40	0.27 ±0.09[a]	0	0.31
	Sr 380980	0.65	0.36 ±0.11[a]	0	0.14
	Sr 380990	0.6	3.4 ±2.4	0	0.68
	Sr 381000	1.046	5.0	0	0.04
	Y 390971	1.11	0.06 ±0.02[b]	0	0.05
	Y 390970	3.7	0.33	0	0.97
	Y 390981	0.65	3.44 ±0.95[b]	0	2.16
	Y 390980	2.0	0.54	0	1.10
	Y 390990	1.4	1.2 ±0.8	0	1.60
	Y 391000	0.756	5.5	0	1.67
	Zr 401040	3.783	0.11	0	< 0.01
	Zr 401050	0.559	1.4	0	0.07

	PRECURSOR CS ZZAAAS	HALF-LIFE (s)	Pn (%)	NO. OF SPEC MEAS	% of $\bar{\nu}_d$ U235(T)
	Nb 411030	15.669	0.13	0	0.16
	Nb 411040	1.00	0.71	0	0.30
	Nb 411050	1.80	2.9	0	0.42
	Nb 411060	0.535	5.5	0	0.05
	Mo 421090	1.033	0.53	0	< 0.01
	Mo 421100	1.892	1.3	0	< 0.01
	Tc 431090	50.00	1.7	0	< 0.01
	Tc 431100	0.83	3.1	0	< 0.01
	Ag 471220	1.5	1.4	0	< 0.01
	Ag 471230	0.39	4.6	0	< 0.01
	Cd 481280	0.83	0.11	0	< 0.01
	In 491271	2.0	0.72 ±0.04[a]	0	0.01
	In 491270	3.76	0.72 ±0.04[a]	0	0.01
	In 491280	0.84	0.063±0.008[a]	0	< 0.01
	In 491291	0.99	3.5 ±0.5[a]	0	0.09
C	In 491290	2.5	3.5 ±0.5[a]	1	0.18
C	In 491300	0.58	1.39 ±0.08[a]	1	0.07
	In 491310	0.28	1.66 ±0.19[a]	0	0.03
	In 491320	0.13	4.1 ±0.8[a]	0	0.02
	Sn 501330	1.47	0.02	0	< 0.01
C	Sn 501340	1.04	17.0 ±7.0	1	0.11
	Sn 501350	0.291	8.6	0	< 0.01
	Sb 511341	10.4	0.086±0.012	0	0.01
C	Sb 511350	1.71	14.0 ±2.0	3	1.16
	Sb 511360	0.82	23.0 ±8.0	0	0.20
	Sb 511370	0.284	20.0	0	0.59
C	Te 521360	17.5	0.9 ±0.4	2	0.78
	Te 521370	2.8	2.2 ±0.5	0	0.53
	Te 521380	1.4	5.6 ±1.6	0	0.21
	Te 521390	0.424	6.3	0	0.02
C	I 531370	24.5	7.2 ±0.7	3	13.11
C	I 531380	6.53	2.6 ±0.3	2	2.34
C	I 531390	2.38	10.2 ±0.9	1	5.65
C	I 531400	0.60	22.0 ±6.0	1	2.71
C	I 531410	0.47	39.0 ±13.0	0	0.32
	I 531420	0.196	16.0	0	0.66
	I 531430	0.328	18.0	0	< 0.01
	Xe 541410	1.72	0.043±0.003	0	0.03
	Xe 541420	1.24	0.41 ±0.03	0	0.10
	Xe 541430	0.30	1.2	0	0.03
	Xe 541440	1.00	0.73	0	< 0.01
	Cs 551410	24.9	0.053±0.004	1	0.13
C	Cs 551420	1.69	0.19 ±0.10	2	0.29
C	Cs 551430	1.78	1.6 ±0.2	3	1.34
C	Cs 551440	1.001	2.8 ±0.7	2	0.56
	Cs 551450	0.58	14.0 ±2.0	1	0.46
	Cs 551460	0.335	13.4 ±0.7	1	0.13
	Cs 551470	0.21	25.0 ±3.0	1	< 0.01
	Ba 561470	2.2	5.2 ±0.5[a]	0	0.27
	Ba 561480	-	23.9 ±2.1[a]	0	0.14
	Ba 561490	0.917	0.03	0	< 0.01
	Ba 561500	1.798	0.24	0	< 0.01
	La 571470	10.0	0.5 ±0.17[a]	0	0.26
	La 571490	2.864	0.81	0	0.03
	La 571500	0.648	0.94	0	< 0.01

[a] Measured subsequent to Ref. 1

[b] Change in Pn or uncertainty subsequent to Ref. 1

[c] Nuclides having spectra supplied by Rudstam

TABLE VII

COMPARISON OF DELAYED NEUTRONS PER 100 FISSIONS

Fission Nuclide	$\bar{\nu}_d$ Calculated ENDF/B-V	$\bar{\nu}_d$ Evaluated ENDF/B-V	$\bar{\nu}_d$ TUTTLE 1979[b]	$\bar{\nu}_d$ Selected Measurements	Group Components of $\bar{\nu}_d$ (Calculated %; ENDF/B-V) 1	2	3	4	5	6
Th232F	4.76 ±0.34 (4.51)[a]	5.27	5.31 ±0.23	4.96±0.30[e]	3.6	17.5	16.6	35.6	21.7	4.9
Th232H	3.03 ±0.29 (2.77)	3.00	2.85 ±0.13	3.1 ±0.3[d]	3.8	14.5	16.3	41.3	16.6	7.4
U233T	0.846±0.066 (0.803)	0.74	0.667±0.029	0.66±0.04[e]	6.5	27.3	20.3	34.9	9.5	1.6
U233F	0.916±0.089 (0.870)	0.74	0.731±0.036	0.78±0.08[c]	7.4	27.9	21.1	30.7	11.5	1.3
U233H	0.708±0.095 (0.657)	0.47	0.422±0.025	0.43±0.04[d]	6.9	23.4	21.8	33.5	12.9	1.5
U235T	1.77 ±0.081 (1.66)	1.67	1.621±0.050	1.58±0.07[e]	2.9	22.1	15.9	35.4	19.0	4.6
U235F	1.98 ±0.18 (1.84)	1.67	1.673±0.036	1.71±0.17[c]	2.8	21.3	17.8	35.7	18.8	3.7
U235H	0.978±0.097 (0.902)	0.93	0.927±0.029	0.95±0.08[d]	4.5	22.2	20.2	35.6	15.2	2.3
U236F	2.26 ±0.19 (2.09)	-	2.21 ±0.24	-	2.3	20.3	15.4	36.1	21.7	4.1
U238F	3.51 ±0.27 (3.13)	4.40	4.39 ±0.10	4.12±0.25[e]	1.1	15.7	11.0	36.0	28.9	7.2
U238H	2.69 ±0.21 (2.38)	2.60	2.73 ±0.08	2.83±0.13[d]	1.8	13.6	11.6	37.7	27.9	7.4
Np237F	1.28 ±0.13 (1.15)	-	-	-	3.0	23.8	14.3	35.9	20.2	2.7
Pu239T	0.769±0.058 (0.675)	0.645	0.628±0.038	0.61±0.05[e]	2.9	29.1	14.0	33.3	18.9	1.7
Pu239F	0.724±0.090 (0.612)	0.645	0.630±0.016	0.65±0.06[c]	3.4	26.3	14.4	32.9	20.9	2.2
Pu239H	0.387±0.062 (0.325)	0.430	0.417±0.016	0.43±0.04[d]	6.5	22.2	16.0	33.6	20.2	1.6
Pu240F	0.923±0.11 (0.798)	0.900	0.95 ±0.08	0.88±0.09[e]	2.8	26.7	12.4	34.3	20.7	3.1
Pu241T	1.58 ±0.13 (1.34)	1.62	1.52 ±0.11	1.57±0.15[e]	1.9	23.2	9.6	33.7	26.9	4.7
Pu241F	1.49 ±0.16 (1.24)	1.62	1.52 ±0.11	-	2.1	23.4	10.6	34.4	25.3	4.1
Pu242F	1.41 ±0.14 (1.20)	-	2.21 ±0.26	1.6 ±0.5[c]	2.6	24.7	10.3	34.0	23.5	4.9
Cf252S	0.690±0.092 (0.538)	0.89	-	-	4.6	30.1	9.3	30.3	24.2	1.6

[a] Values in parantheses used only measured Pn values.

[b] May 1979 revision of NSE 56 p.37, 1975 article to be published.

[c] Krick and Evans, NSE 47 p.311 (Here, average values between 0.1 and 1.8 MeV are listed).

[d] C. F. Masters et al. NSE 36 p.202 (High energy values at 14.9 MeV).

[e] G. R. Keepin et al. NSE 6 p.1 (Probable error converted to standard deviation).

755, 865, and 955 keV. These values, being based on 10-keV histograms, are not precise, apart from any other uncertainty.

Average energies for each of the calculated spectra are listed in Table VIII.

The 24 nuclides having spectra in these calculations are identified in Table VI. These account for approximately 78% of the total $\bar{\nu}_d$ emission. One interesting feature of the calculations is that while $\bar{\nu}_d$ varies by almost a factor of 2 between thermal and 14 MeV, the spectral shape is nearly constant with fission neutron energy. The shape does differ for different fissionable nuclides. Figure 7 shows the shape for ^{239}Pu fission. Another feature not shown in these figures is the presence of an unexpected, large peak at approximately 1.8 MeV; this may require additional experimental verification.

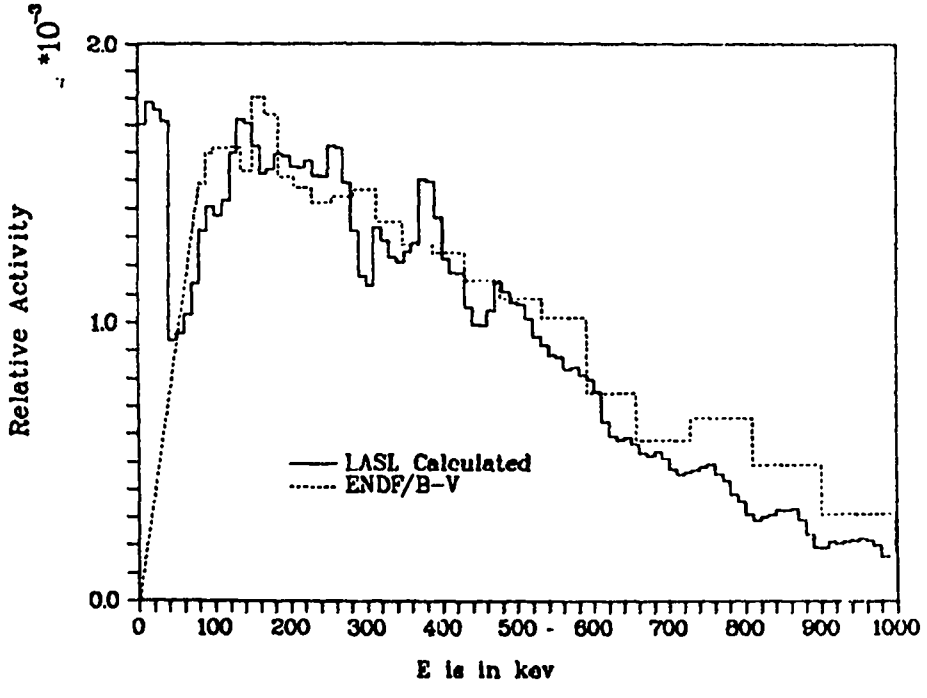

Fig. 6.
Calculated $\bar{\nu}_d$ spectra compared to ENDF/B-V evaluation for ^{235}U (fast fission).

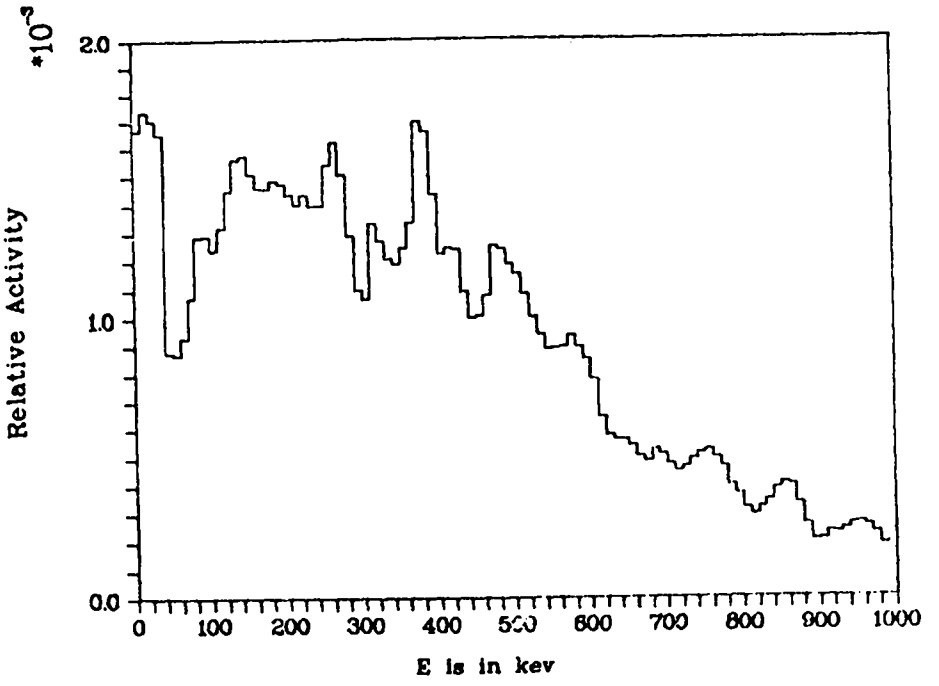

Fig. 7.
Calculated $\bar{\nu}_d$ spectra for ^{239}Pu (fast fission).

TABLE VIII

AVERAGE $\bar{\nu}_d$ ENERGIES FROM CALCULATED SPECTRA

Fissionable[a] Nuclide	$\bar{E}$ keV	Fissionable[a] Nuclide	$\bar{E}$ keV
Th232(F)	408	U238(H)	414
TH232(H)	405	Np237(F)	412
U233(T)	400	Pu239(T)	416
U233(F)	391	Pu239(F)	414
U233(H)	382	Pu239(H)	396
U235(T)	394	Pu241(F)	405
U235(F)	400	Pu241(T)	414
U235(H)	393	Pu241(F)	419
U236(F)	403	Pu242(F)	422
U238(F)	413	Cf252(S)	425

[a] T = thermal, F = fast, H = 14 MeV, and S = spontaneous

B. Calculations in Support of LASL Non-Destructive Assay Methods (W. B. Wilson, R. J. LaBauve, and T. R. England)

LASL Group T-2 is currently providing support to LASL Group Q-5 (International Safeguards) in a program leading to the definition of measurable reactor spent-fuel properties accurately revealing fuel-irradiation history and nuclide inventory. The initial T-2 effort has centered on the demonstration of validity of codes and data in the calculation of benchmark spent-fuel isotopes. This capability has required the interfacing of the EPRI-CELL[19] and EPRI-CINDER codes,[12,20] which was accomplished as follows.

1. Coding updates to the EPRI-Cell code have been completed to write a file of time-step data important to EPRI-CINDER calculations. CELL contains a CINDER module to trace most actinide nuclides from ^{234}U to ^{241}Am, as well as lumped fission products. The data written to the file include the dimensions of the fuel-rod regions and initial nuclide number densities. Data written for each timestep include:
   - Four-group flux values in each fuel region.
   - Nuclide densities of selected actinides in each fuel region.
   - Four-group cross sections [absorption, fission and (n,2n)].
   - Time-step length.
2. Coding of the small PHAZE interface code (approximately 150 lines) has been completed and tested. PHAZE reads the file described in (1) above plus problem-descriptive information. The code prepares an input file for a single region of the fuel, including time-step cards with 4-group region fluxes and initial number density cards. The code also prepares time-step cross-section input for the desired region. Alternatively, the code will determine average cross-section and flux data to describe the combined fuel from regional values.
3. Coding changes to the EPRI-CINDER code have been completed to read a problem-independent data library from one file and problem-dependent data from another file. The code requires no correspondence of libraries from CELL to CINDER. The code also computes coupling cross sections from time-step data where (n,2n) reactions occur in the chain structure.
4. The EPRI-CINDER data library has been changed to separate problem-independent data into a single file consistent with (3) above.

Tandem EPRI-CELL/PHAZE/EPRI-CINDER calculations have been performed for 3.1% enriched PWR fuel exposed to approximately 24 500 MWd/t. The PHAZE code

was used to prepare an EPRI-CINDER input file for each fuel region and, by averaging regional flux and cross-section values, an input file for the fuel average. Five EPRI-CINDER calculations corresponding to the five input files described above were performed to determine regional and average nuclide inventories and nuclide ratios. The agreement between the single fuel-average calculation and the average of the four-region calculations is excellent. This serves to demonstrate the validity of fuel-average calculations.

Two benchmark samples of 2.56% enriched H. B. Robinson-2 fuel[21] were calculated by the code sequence described above using the fuel-average properties in EPRI-CINDER. The samples of rod P8, bundle B05 from cycles I and II were calculated using 35-step histogram power histories yielding CELL-calculated exposure values corresponding to those quoted for the samples. It was found that CELL-calculated burnup (atom-percent-fission) values were considerably lower than those quoted for the samples. This discrepancy is due to the difference in the recoverable energy per fission value calculated and used by CELL and the lower (approximately 204.8 MeV) implicit in the ASTM conversion of measured burnup to exposure: 1 atom percent fission = 96000 $\pm$ 300 MWd/t. Measured and calculated isotope ratios for the two samples are given in Table IX.

EPRI-CINDER has now been modified to write a summary file of nuclide properties and densities. A small utility code RATIOS has been completed to list nuclide ratios as a function of exposure or cooling time.

C. EPRI-CINDER Library for Long-Term Actinide Decay [W. B. Wilson, T. R. England, and D. E. Wessol (EG&G, Idaho)]

Previous calculations[22] have demonstrated that actinide nuclides account for a considerable fraction of radioactive decay power in LWR fuel following shutdown. Beyond cooling times of approximately 60 years, decay power is dominated by actinides.[13] The calculation of actinide decay power, neutron source strength, and/or decay spectra requires the temporal description of all daughter products of the generally long-lived actinides formed during fuel irradiation.

The decay paths for all actinides end ultimately with the stable nuclides ^{206}Pb, ^{207}Pb, ^{208}Pb, or ^{209}Bi. The complete description of all decay products from ^{246}Cm and lower mass nuclides requires 173 linear chains to describe the 93 individual nuclides explicitly. The calculation of actinide ensemble properties permits the implicit treatment of 38 of the short-lived decay products by adding decay effects to long-lived parent nuclides explicitly included, reducing the number of linear chains to 32.

TABLE IX

H. B. ROBINSON-2 SAMPLES P8a AND P8b
COMPARISON OF MEASURED ATOM RATIOS WITH VALUES
CALCULATED WITH EPRI-CELL/EPRI-CINDER, USING
DETAILED POWER HISTORIES

	ATOM RATIOS			
	Sample P8a 4570 MWd/t		Sample P8b 30920 MWd/t	
Ratio	Measured	Calculated	Measured	Calculated
$^{234}U/U$	0.00016	0.00015	0.00014	0.00013
$^{235}U/U$	0.00816	0.00864	0.00612	0.00629
$^{236}U/U$	0.00326	0.00314	0.00352	0.00347
$^{238}U/U$	0.98842	0.98807	0.99022	0.99010
$^{238}Pu/Pu$	0.01143	0.00950	0.01676	0.01373
$^{239}Pu/Pu$	0.59557	0.60207	0.54261	0.54642
$^{240}Pu/Pu$	0.23290	0.22534	0.25101	0.23860
$^{241}Pu/Pu$	0.11842	0.11809	0.12998	0.13155
$^{242}Pu/Pu$	0.04168	0.04501	0.05964	0.06969
$^{239}Pu/^{238}U$	0.00494	0.00486	0.00518	0.00497
$^{148}Nd/^{238}U$	0.000450	0.000450	0.000570	0.000567

The production of the reduced 32-chain actinide decay library is approximately 25% complete. ENDF/B-V contains decay data for only 42 of the 87 radioactive nuclides. Additional decay data have been obtained from Walker[23] and other sources. Data provided by Ombrellaro and Johnson[24] on (α,n) and spontaneous fission neutron production are being incorporated for neutron-source calculations.

REFERENCES

1. W. R. Arnold, J.A. Phillips, G. A. Sawyer, E. J. Stovall, Jr., and J. L. Tuck, "Cross Sections for the Reactions D(d,p)T, D(d,n)He^3, T(d,n)He^4, and He^3(d,p)He^4 Below 120 keV," Phys. Rev. 93, 483 (1954).

2. E. D. Arthur and P. G. Young, "Calculation of Neutron Cross Sections on Iron Between 3 and 40 MeV," Internl. Conf. on Nuclear Cross Sections for Technology, Knoxville, TN (Oct. 1979).

3. F. G. Perey, "Optical Model Analysis of Proton Elastic Scattering in the Range of 9 to 22 MeV," Phys. Rev. 131, 745 (1962).

4. O. F. Lemos, "Diffusion Elastique de Particules Alpha de 21 a 29.6 MeV sur des Noyaux de la Region Ti-Zn,: Orsay report, Series A136 (1972).

5. C. M. Lederer and Virginia Shirley, Table of Isotopes, Seventh Edition, (John Wiley and Sons, New York, 1978).

6. R. J. Peterson, "Inelastic Scattering of 17.5 MeV Protons from ^{51}V, ^{52}Cr, ^{55}Mn, and ^{50}Fe," Ann. of Phys. 53, 40 (1969).

7. David G. Madland and J. Rayford Nix, "Calculation of Prompt Fission Neutron Spectra," Bull. Am. Phys. Soc. 24, 885 (1979), and contributed paper to the Proc. of the Internl. Conf. on Nuclear Cross Sections for Technology, Knoxville, TN (Oct. 1979).

8. D. R. Harris, R. G. Fluharty, J. J. Koelling, and N. L. Whittemore, "Medium and Low-Energy Neutron Cross-Section Library," Trans. Am. Nucl. Soc. 15, 958 (1972).

9. D. G. Foster, Jr., and D. R. Harris, "NASA Extension of the Medium Energy Nuclear Data Library to 3.5 GeV," in "Applied Nuclear Data Research and Development Quarterly Progress Report January 1 through March 31, 1974," Los Alamos Scientific Laboratory report LA-5655-PR (1974), p. 21.

10. D. G. Foster, Jr., G. M. Hale, W. B. Wilson, and D. R. Harris, "Medium Energy Library," in "Applied Nuclear Data Research and Development Quarterly Progress Report July 1 through September 30 1974," Los Alamos Scientific Laboratory report LA-5804-PR (1974), p. 20. See also "Applied Nuclear Data Research and Development Quarterly Progress Report October 1 through December 31, 1974," Los Alamos Scientific Laboratory report LA-5944-PR (1975), p. 13, and "Applied Nuclear Data Research and Development Quarterly Progress Report October 1 through December 31, 1975," Los Alamos Scientific Laboratory report LA-6266-PR (1976), p. 16.

11. T. R. England, "CINDER--A One-Point Depletion and Fission Product Program," Westinghouse report WAPD-TM-334 (June 1964).

12. T. R. England, W. B. Wilson, and M. G. Stamatelatos, "Fission Product Data for Thermal Reactor, Part 2, Users Manual for EPRI-CINDER Code and Data," Electric Power Research Institute report EPRI NP-356, Part 2 (December 1976). (Also published as Los Alamos Scientific Laboratory report LA-6746-MS (December 1976).

13. T. R. England and W. B. Wilson, "TMI-2 Decay Power: LASL Fission-Product and Actinide Decay Power Calculations for the President's Commission on the Accident at Three Mile Island," Los Alamos Scientific Laboratory report LA-8041-MS (Oct. 1979).

14. "American NAtional Standards Institute/American Nuclear Society Standard, Decay Heat Power in Light Water Reactors," ANS-5.1 (1979).

15. See Proceedings of the Second Advisory Group Meeting on Fission Product Nuclear Data, Petten, Netherlands (Sept. 1977), IAEA-213.

16. Proc. of Consultants Meeting on Delayed Neutron Properties, Vienna (March 1979) INDC(NDS)-107/G4 Special.

17. T. R. England, R. E. Schenter, and F. Schmittroth, "Delayed Neutron Calculations, Using ENDF/B-V Data," presented at Internl. Conf. on Nuclear Cross Sections for Technology, Knoxville, TN (Oct. 1979).

18. Gösta Rudstam, Studsvik, personal communication.

19. "ARMP: Advanced Recycle Methodolgy Program," Electric Power Research Institute report CCM-3 (Sept. 1977) (Proprietary) Chapt. 5, Part II, "EPRI-CELL Code Description."

20. T. R. England, W. B. Wilson, and M. G. Stamatelatos, "Fission Product Data for Thermal Reactors, Part 1: A Data Set for EPRI-CINDER Using ENDF/B-IV," Electric Power Research Institute report EPRI NP-356, Part 1 (Dec. 1976). Also published as Los Alamos Scientific Laboratory report LA-6745-MS (Dec. 1976).

21. A. A. Bauer, L. M. Lowry, and J. S. Perrin, "Progress on Evaluating Strength and Ductility of Irradiated Zircaloy During July through September 1975," Battelle Columbus Laboratories report BMI-1938 (1975).

22. W. B. Wilson, T. R. England, O. Ozer, and D. E. Wessol, "Actinide Decay Power," Trans. Am. Nucl. Soc. 32, 737 (1979).

23. W. Walker, Atomic Energy of Canada, LTD., personal communication on actinide nuclide decay energies.

24. P. A. Ombrellaro and D. L. Johnson, "Subcritical Reactivity Monitoring: Neutron Yields from Spontaneous (α,n) Reactions in FFTF Fuel," Hanford Engineering Development Laboratory report HEDL TME 78-39 (June 1978).

Printed in the United States of America. Available from
National Technical Information Service
US Department of Commerce
5285 Port Royal Road
Springfield, VA 22161

Microfiche $3.00

001-025	4.00	126-150	7.25	251-275	10.75	376-400	13.00	501-525	15.25
026-050	4.50	151-175	8.00	276-300	11.00	401-425	13.25	526-550	15.50
051-075	5.25	176-200	9.00	301-325	11.75	426-450	14.00	551-575	16.25
076-100	6.00	201-225	9.25	326-350	12.00	451-475	14.50	576-600	16.50
101-125	6.50	226-250	9.50	351-375	12.50	476-500	15.00	601-up	

Note: Add $2.50 for each additional 100-page increment from 601 pages up.